Modeling and perspectives of the Si nanocrystals–Er interaction for optical amplification

Domenico Pacifici, Giorgia Franzò, and Francesco Priolo
INFM and Dipartimento di Fisica e Astronomia, Via Santa Sofia 64, I-95123 Catania, Italy

Fabio Iacona
CNR-IMM, Sezione di Catania, Stradale Primosole 50, I-95121 Catania, Italy

Luca Dal Negro
INFM and Dipartimento di Fisica, Via Sommarive 14, I-38050 Povo, Trento, Italy
(Received 12 November 2002; published 4 June 2003)

In the present article, a detailed study of the optical properties of the Er-doped Si nanocrystals system, obtained through ion implantation of Er in samples containing Si nanocrystals formed by plasma enhanced chemical vapor deposition is reported. In particular, we present a phenomenological model based on an energy level scheme taking into account the strong coupling between each Si nanocrystal (NC) and the neighboring Er ions, and considering the interactions between pairs of Er ions too, such as the concentration quenching effect and the cooperative up-conversion mechanism. Based on this model, we wrote down a system of coupled first order differential rate equations describing the time evolution of the population of both the Si NC and the Er related excited levels. By studying the steady state and time resolved luminescence signals at both the 1.54 and 0.98 μm Er lines and at the Si nanocrystals emission (at around 0.8 μm), we were able to fit the experimental data in a wide range of Er concentration (between $3\times10^{17}/\mathrm{cm}^3$ and $1.4\times10^{21}/\mathrm{cm}^3$) and excitation pump power (in the range $1-10^3$ mW), determining a value of 3×10^{-15} $\mathrm{cm}^3\,\mathrm{s}^{-1}$ for the coupling constant describing the interaction between Si NC and Er ions, and of 7×10^{-17} $\mathrm{cm}^3\,\mathrm{s}^{-1}$ for the cooperative up-conversion coefficient. Moreover, an energy transfer time of ~1 μs has been estimated, confirming that Si nanocrystals can actually play a crucial role as efficient sensitizers for the rare earth. In addition, the role of Si nanocrystals and of strong gain limiting processes, such as cooperative up-conversion and confined carriers absorption from an excited NC, in determining positive gain at 1.54 μm will be investigated in details. The impact of these results on the fabrication of optical amplifiers will be finally addressed.

DOI: 10.1103/PhysRevB.67.245301 PACS number(s): 78.55.−m, 78.66.−w, 78.20.Bh, 81.15.Gh

I. INTRODUCTION

Among the different approaches developed to overcome the intrinsic low efficiency of silicon as a light emitter, quantum confinement and rare earth doping of silicon have dominated the scientific scenario of silicon-based microphotonics. Indeed, due to their promising optical properties, all kind of silicon nanostructures, i.e., porous silicon,[1,2] Si nanocrystals (NC's) embedded in SiO_2 matrix,[3–11] and Si/SiO_2 superlattices[12–15] have been widely studied. The efficient, tunable in the visible, room-temperature light emission of all of these structures has been ascribed to the recombination of a quantum confined exciton[2,16,17] which is self-trapped[18,19] in a size dependent Si=O level[20] at the interface between the Si nanostructure and the SiO_2 matrix. On the other hand, studies on Er doped crystalline Si have demonstrated that Er can be efficiently excited in Si through electron-hole pair recombination or through impact of energetic carriers[21,22] and, despite the equally efficient nonradiative deexcitation processes such as Auger with free carriers and energy back transfer,[21] Er-doped Si devices operating at room temperature have been developed[22,23]. Recently, Er doping of Si nanocrystals has been recognized as an interesting way of combining the promising features of both the previous methods.[24–31] Indeed, it has been demonstrated that Si NC's in presence of Er act as efficient sensitizers for the rare earth.[30–34] In particular, the NC, once excited, promptly transfers quasiresonantly[35] its energy to the nearby Er ion, which then decays emitting a photon at 1.54 μm. The effective excitation cross section for Er in presence of Si NC's is more than two orders of magnitude higher with respect to the resonant absorption of a photon in a silica matrix.[30] Moreover the nonradiative deexcitation processes are strongly suppressed, the Er lifetime being almost constant in the temperature range between 11 and 300 K (Ref. 36). The recent determination of net optical gain at 1.54 μm in Er-doped Si nanocluster sensitized waveguides[40–42] and the demonstration of efficient room-temperature electroluminescence from Er-Si NC devices[37] opened the route towards the future fabrication of electrically driven optical amplifiers based on this system. Several basic issues remain, however, to be addressed first, namely, the role and strength of the competitive nonradiative processes, the coupling strength between Si NC's and Er ions and the microscopic details of the interaction.

In the present work, a rate equation model describing the time evolution of the coupled Er and Si NC level populations will be presented and an estimate of the efficiency of the energy transfer will be reported. In particular, the occurrence of cooperative up-conversion among interacting Er ions in presence of Si NC's will be demonstrated for the first time to our knowledge. Through a comparison of simulated and measured photoluminescence data in a wide range of Er concentrations and pump powers, both the coupling and the up-conversion coefficients will be determined. Important issues

such as the maximum number of excitable Er ions per NC, and the role of up-conversion and carrier absorption from an excited nanocrystal in limiting the possibility of obtaining positive gain at the 1.54 μm Er related emission will be addressed. These data will be reported, a comparison with recent results[38–42] will be made and future perspective towards the achievement of optical amplifiers will be discussed.

II. EXPERIMENT

Si nanocrystals were produced by high temperature annealing of a 0.2 μm thick substoichiometric SiO_x film (with 42 at. % Si) grown by plasma enhanced chemical vapor deposition (PECVD) on top of a Si substrate. Thermal treatments were performed at 1250 °C for 1 h in ultrapure nitrogen atmosphere. The annealing process induces the separation of the Si and SiO_2 phases, leading to the formation of uniformly distributed Si NC's with a mean radius of 1.7 nm, as evidenced by plan view transmission electron microscopy (TEM). The estimated Si NC density in the sample has a value of $\sim 1\times 10^{19}/cm^3$. After the Si NC formation, Er ions were then implanted at different energies (in the range between 170–500 keV) and doses in order to produce an almost constant Er concentration (in the range $3\times 10^{17}-1.4\times 10^{21}/cm^3$) all over the film thickness. Correspondingly, the mean number of Er ions per NC varies in the range 0.03–140. The very same Er implants were also performed in SiO_2 layers not containing Si NC's in order to have reference samples. All of the samples were eventually annealed at 900 °C for 1 h in ultrapure nitrogen atmosphere in order to remove the residual damage left over by the implantation process[43] and to activate Er, preventing it from clustering.

Photoluminescence (PL) measurements were performed by pumping with the 488 nm line of an Ar laser. The pump power was varied in a wide range, between $1-10^3$ mW, and focused over a circular area of $\sim$0.3 mm in radius. The laser beam was chopped through an acousto-optic modulator at a frequency of 11 Hz. The luminescence signal was analyzed by a single grating monochromator and detected by a photomultiplier tube for the visible range (0.4–0.9 μm) or by a Ge detector for the infrared (0.8–1.7 μm spectral region). Spectra were recorded with a lock-in amplifier using the chopping frequency as a reference. All the spectra have been measured at room temperature and corrected for the spectral system response. Time resolved PL measurements were performed by first detecting the modulated luminescence signal with a Hamamatsu photomultiplier tube (model R5509-72) having an almost constant spectral response in the range 0.4–1.7 μm. The signal was hence analyzed with a photon counting multichannel scaler, triggered by the acousto-optic modulator. The overall time resolution of our system is of $\sim$5 ns.

III. EXPERIMENTAL EVIDENCES

In Fig. 1, the room temperature PL spectra of three different samples consisting of Er in presence of Si NC's (continuous lines), Er in SiO_2 (dashed line), and Si NC's before Er implantation (short-dashed line) are shown. The Er concentration in the two implanted samples is $6.5\times 10^{20}/cm^3$ and, due to the multiple implants, is constant all over the film thickness. It is worth noticing that all of the spectra have been obtained in the very same conditions, i.e., exciting the systems with the 488 nm Ar-laser line at a pump power of 100 mW and at a chopper frequency of 11 Hz. Moreover all of the spectra have been corrected for the spectral system response, as obtained through a calibrated lamp. Hence the ratio of the intensities at the various wavelengths is an absolute value.

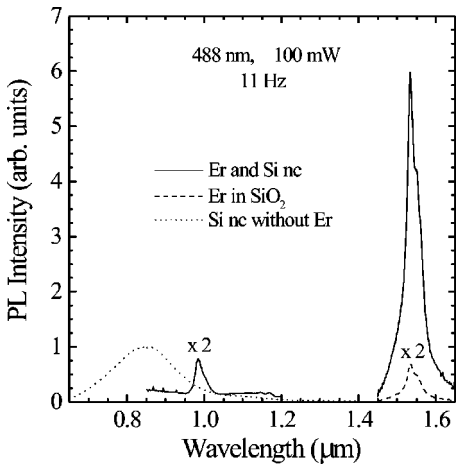

FIG. 1. Room temperature photoluminescence (PL) spectra of Si nanocrystals (short-dashed line), Er in SiO_2 (dashed line) and Er in presence of Si NC's (continuous lines). The Er concentration in the two implanted samples is $6.5\times 10^{20}/cm^3$.

A lot of information can be gained from Fig. 1. First of all, it is worth noticing that the efficient luminescence at around 0.8 μm due to Si NC's alone completely disappears when introducing Er in the sample. Indeed, an intense peak at 1.54 μm from Er^{3+} ions appears at the expenses of the Si NC related emission, thus suggesting that the energy is now redistributed in the sample, being preferentially transferred from Si NC's to the rare earth. Moreover, the 1.54 μm PL intensity due to Er ions in presence of Si NC's is over one order of magnitude higher with respect to the sample with Er in SiO_2. It has been demonstrated that this intensity increase is due to the sensitizing action made by Si NC's for the Er ion.[30] In fact, each Si NC absorbs an incident photon and, once excited, promptly transfers its energy to a nearby Er ion which will return to its ground state emitting a photon at 1.54 μm, corresponding to the transition from the first excited level $^4I_{13/2}$ to the ground state $^4I_{15/2}$ of Er^{3+}. The measured effective excitation cross section for the Si NC mediated excitation process of Er is $\sim 2\times 10^{-16}$ cm^2, comparable to the value found for isolated Si NC's, and three orders of magnitude higher than the value of $\sim 1\times 10^{-19}$ cm^2 for the excitation of Er through the direct absorption of an incident photon (which is typical for Er in an insulating host). Moreover, since it has been demonstrated that the high resolution Er-related spectra in the two matrices have similar shapes,[31] and since the shapes are closely related to the local environment, it has been concluded that the emitting Er ions in presence of Si NC are surrounded, at least in a first neighbors approxi-

mation, by oxide.[31] In addition we have shown that the nonradiative decay processes are quite reduced.[28,31,36] Therefore, thanks to the strong sensitizing action of Si NC's and to the reduced nonradiative decay channels, the Er-doped Si NC system is a quite promising light emitter candidate.

As can also be seen in Fig. 1, the 1.54 μm luminescence intensity coming from Er in presence of Si NC's is even more intense than the 0.8 μm luminescence signal due to Si NC's without Er. Another important feature shown in Fig. 1 is the presence of the 0.98 μm line in the spectrum related to the Er-doped Si NC sample, due to the radiative transition from the second excited state $^4I_{11/2}$ to the ground state $^4I_{15/2}$ of Er. This is a clear evidence of the energy transfer between Si NC's and Er ions, since it has been postulated[28] and recently demonstrated[35] that a quasiresonant energy transfer can occur between the Si NC's emitting at 0.8 and 0.98 μm and the two manifold Er-related levels $^4I_{9/2}$ and $^4I_{11/2}$, respectively. Thus the appearance of the efficient 0.98 μm Er line can again be attributed to the sensitizing action of Si NC's which are strongly coupled with the Er-related levels. Indeed this line is still visible at room temperature even at laser pump powers as low as a few mW, being in that range totally undetectable for the Er-doped silicon dioxide sample.

The experimental facts can be summarized as follows.

(i) In presence of Si NC, Er ions are excited through the NC's themselves which act as the absorbing system.

(ii) The energy transfer occurs quasiresonantly[35] from the Si NC's to the $^4I_{9/2}$ Er manifold for Si NC's emitting at $\sim$0.8 μm.

(iii) The effective excitation cross section for Er is enhanced by $\sim$3 orders of magnitude by the sensitizing action of Si NC's,[30] with respect to Er in insulating hosts.

(iv) The effective excitation cross section for Er in presence of Si NC is comparable to the absorption cross section of isolated Si NC's, thus attesting the strong coupling between Si NC's and Er.

(v) Er is surrounded by O and it is very likely within the oxide matrix or at the Si NC/oxide interface.[31]

(vi) The decay channels, typically limiting the efficiency of Er emission in crystalline Si (Ref. 21), are absent in this case.[28,31,36]

IV. MODELING THE Si-NANOCRYSTAL–Er INTERACTION

In order to explain the overall experimental picture, we developed a model for the Si-NC–Er interaction, based on the schematic energy levels diagram reported in Fig. 2. In this scheme a Si NC is represented by a three level system, consisting of two band edge levels and of an interfacial level, which acts as a trap for the exciton.[18–20] Since the trapping is assumed to be a very fast process if compared to the typical decay times, we commit a small error for our purposes in considering the Si NC as an effective two levels system, where the ground state is represented by level a and the excited state by level b. Thus σ_{ab} is the effective excitation cross section describing the creation of an exciton and its subsequent fast trapping at the interfacial level, following the absorption of a 488 nm photon. w_b is the total recombination

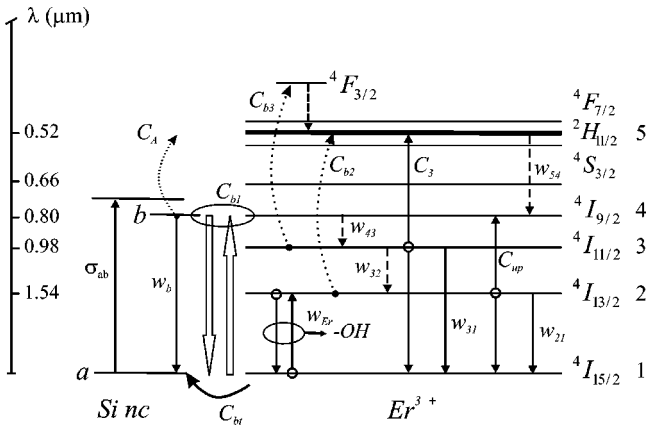

FIG. 2. Energy level scheme for the system of interacting Si NC's and Er ions. The Si NC can be represented by a two-effective energy level diagram. Er^{3+} ions can be thought of as a five-energy-level system. Si NC's having different sizes can be coupled with both the $^4I_{9/2}$ and $^4I_{11/2}$ levels.

rate of an exciton for the isolated Si NC, comprising both radiative and nonradiative recombination rates. Er^{3+} is schematized as a five levels system, where the fifth level is the sum of $^4S_{3/2}$, $^2H_{11/2}$, and $^4F_{7/2}$, which are strongly overlapping, due to the Stark splitting caused by the matrix field on each multiplet, and can therefore be treated as a single level. With w_{ij} we indicate the total transition rate from level i to level j, where $i,j=1,2,\ldots,5$ and $i>j$.

Many of the parameters shown in Fig. 2 are well known experimentally or theoretically, others deserve a detailed study in order to be determined. One of the most important coefficients is C_{b1}, since it describes the coupling between the excited Si NC level and the ground state of Er, and it is therefore responsible for the energy transfer between the Si NC's and the rare earths surrounding it. This energy transfer is indeed represented by the two white arrows, depicting the nonradiative deexcitation of an excited Si NC (down arrow) and the following Er^{3+} excitation to the $^4I_{9/2}$ level (up arrow). C_{bi} $(i\geqslant 2)$ describes the excited state excitation (ESE) from level i. This process is very similar to the excited state absorption of a photon from an excited level of Er in insulating matrices. In this case, ESE describes the reexcitation of an excited Er level through the energy transfer from an excited Si NC. After Er is excited to the $^4I_{9/2}$ level, an energy back transfer from this level back to the first excited level of a NC could occur and the strength of this process is given by C_{bt}. However, the back transfer mechanism is quite ineffective, since level $^4I_{9/2}$ is efficiently depleted by a very fast relaxation to level $^4I_{11/2}$, being therefore almost empty.

Another effect which we should take into account is very similar to the Auger effect occurring in Er-doped crystalline Si (Ref. 21), where the energy of an excited level of Er can be given up to a carrier (electron or hole) which is free in the conduction or valence band of bulk Si, promoting it to a higher lying level. In the Er-Si NC system, it could happen that the energy can be transferred from an excited Er level back to a confined exciton, thus promoting it to a higher energy level. This process is represented by the constant C_A, taking into account the Auger process with both the electron

or the hole forming the exciton. Clearly, this Auger process, in order to occur, requires that a new exciton is formed in the NC while an excited Er level is still filled. Therefore it becomes effective only at high pump powers and it mainly involves the long lived $^4I_{13/2}$ level. Moreover, due to the quantized nature of both the excitonic and the Er related levels, the Auger effect with the nanostructure should be less efficient than in bulk Si, where a continuum of densely spaced energy levels in both the valence and the conduction bands exists.

We also take into account the concentration quenching effect, which is due to the energy migration all over the sample caused by the energy transfer between two nearby Er ions, one in the first excited level and the other in the ground state. Concentration quenching has been well characterized in a previous work,[30] and therefore the value of the total rate of deexcitation from the first excited Er level, i.e., $w_{21}+w_{\mathrm{Er}}$, where w_{Er} takes into account the concentration quenching effect, is well known. Indeed, $w_{21}=4.2\times10^2\ \mathrm{s}^{-1}$ and $w_{\mathrm{Er}}=8\pi C_{\mathrm{Er}}N_qN_0$, where N_q is the concentration of quenching centers (probably $-$OH groups), C_{Er} is the coupling coefficient describing the interaction between the first excited and the ground levels of Er, and N_0 is the total Er cocentration. From experiments[30] we get $C_{\mathrm{Er}}N_q=3.2\times10^{-20}\ \mathrm{cm}^3\,\mathrm{s}^{-1}$.

Eventually, the constants C_{up} and C_3 are the cooperative up-conversion coefficients describing the interaction of two nearby Er ions which are both in the first or in the second excited states, respectively. In the first case one of the two ions will return to the ground state giving its energy to the other which will be excited to the $^4I_{9/2}$ level. In the second case the interaction will bring one ion to the $^2H_{11/2}$ level and the other to the ground state. In the model we take also into account the possibility of a direct absorption of a 488 nm photon by Er leading to a transition from the ground state to the $^4F_{7/2}$ level. This process is characterized by an excitation cross section of $\sim1\times10^{-19}\ \mathrm{cm}^2$, as determined in an oxide reference sample.

Thanks to this scheme, we are able to write down the set of first order rate equations describing the time evolution of the concentration of Si NC's and Er ions in each level:

$$\frac{dn_b}{dt}=\sigma_{ab}\phi n_a-w_bn_b-\sum_{i=1}^{3}C_{bi}n_bN_i,$$

$$\frac{dn_a}{dt}=-\sigma_{ab}\phi n_a+w_bn_b+\sum_{i=1}^{3}C_{bi}n_bN_i,$$

$$\frac{dN_5}{dt}=\sigma\phi N_1+\sum_{i=2}^{3}C_{bi}n_bN_i+C_3N_3^2-(w_{51}+w_{54})N_5,$$

$$\frac{dN_4}{dt}=C_{b1}n_bN_1+C_{\mathrm{up}}N_2^2+w_{54}N_5-w_{43}N_4, \qquad (1)$$

$$\frac{dN_3}{dt}=w_{43}N_4-(w_{32}+w_{31})N_3-C_{b3}n_bN_3-2C_3N_3^2,$$

$$\frac{dN_2}{dt}=w_{32}N_3-(w_{21}+w_{\mathrm{Er}})N_2-2C_{\mathrm{up}}N_2^2-C_{b2}n_bN_2-C_An_bN_2,$$

$$\frac{dN_1}{dt}=(w_{21}+w_{\mathrm{Er}})N_2+C_{\mathrm{up}}N_2^2+C_An_bN_2+w_{31}N_3+C_3N_3^2+w_{51}N_5-\sigma\phi N_1-C_{b1}n_bN_1,$$

where ϕ is the flux of photons incident onto the sample, $n_{a,b}$ and N_i, with $i\geqslant1$, are the density level populations of Si nanocrystals and of Er ions, as represented in Fig. 2. In particular, we can define $n_a+n_b=n_0$ and $\Sigma_iN_i=N_0$, where n_0 and N_0 are the total concentrations of excitable Si NC's and Er ions, respectively. Here we assume that each NC contains at maximum one exciton at a time, since the Auger effect between two excitons would lead to a quick ($<$ns) recombination of one of them, thus leaving only one exciton inside the NC in times much smaller than the typical times characterizing the Er system. Therefore talking about an excited nanocrystal we are simply referring to a NC with an exciton in it. A NC with no excitons, i.e., not excited, will be referred to as a NC in the ground level *a*. It is worth noticing that the interaction between two levels is represented in Eq. (1) through terms involving the product of the concentrations of the centers which are actually lying in those levels. Therefore the interaction probability will be described by rates which are inversely proportional to the square of the mean interaction volumes. In such a way we are introducing a short-range (dipole-dipole-like) interaction whose strength inversely depends on the sixth power of the mean distance between the two centers. On the other hand, we notice that the nonradiative deexcitation rates in Er^{3+} from higher lying levels to closely spaced lower levels are quite high. In particular $w_{54},w_{43}\gg w_{32}\gg w_{21}$.

A few comments need to be made at this stage. Indeed, through Eq. (1) we are taking into account many phenomena which could in principle occur in the Er-doped Si nanocrystal system. Actually, among the various processes, we can distinguish between first and second order mechanisms, depending on the weight of the terms in the rate equation system (1). As far as the Er ion is concerned, it is evident, for example, that the most important mechanisms are the primary excitation due to the presence of Si nc, described by a term containing C_{b1}, and all the processes involving the long-lived level $^4I_{13/2}$, such as cooperative upconversion between two neighboring Er ions excited in that level, excited state excitation, concentration quenching, and eventually Auger processes with a nearby exciton. Indeed, mechanisms involving the interaction between two levels, bring in Eq. (1) a term which is proportional to the product of the population densities of the two levels. Therefore, the more a level is populated the stronger is its influence in the system of rate equations (1). Since the longer is the lifetime of a level the more that level is populated, we gain the result that excited Er levels other than the first one are much less important in the kinetics of the system, since they are almost empty, being characterized by lifetimes $\lesssim1\ \mu$s, i.e., very small if com-

TABLE I. Physical parameters taken from Ref. 30 or as determined by a best fit of the overall experimental data, by using Eq. (1).

Symbol	Value	Reference
λ_{exc}	488 nm	
σ_{ab}	2×10^{-16} cm^2	Ref. 30
σ	1×10^{-19} cm^2	Ref. 30
w_b	2×10^{4} s^{-1}	Ref. 30
w_{21}	4.2×10^{2} s^{-1}	Ref. 30
$w_{Er}=8\pi C_{Er}N_qN_0$	$8.1\times10^{-19}N_0$s^{-1}	Ref. 30[a]
w_{32}	4.2×10^{5} s^{-1}	this work[b]
w_{43}	$\sim1\times10^{7}$ s^{-1}	this work
w_{54}	$<1\times10^{7}$ s^{-1}	this work[c]
C_{b1}	3×10^{-15} cm^3 s^{-1}	this work
C_{up}	7×10^{-17} cm^3 s^{-1}	this work
C_{b2}	$<3\times10^{-19}$ cm^3 s^{-1}	this work[c]
C_{b3}	$<3\times10^{-19}$ cm^3 s^{-1}	this work[c]
C_{bt}	$<3\times10^{-19}$ cm^3 s^{-1}	this work[c]
C_A	$<3\times10^{-19}$ cm^3 s^{-1}	this work[c]
C_3	$\sim7\times10^{-17}$ cm^3 s^{-1}	this work

[a]N_0 is the total Er concentration expressed in cm^{-3}.
[b]$w_{32}\sim3\times10^2 w_{31}$.
[c]Upper limit determined within the present experimental data set.

pared to the value of ~1 ms related to the $^4I_{13/2}$ level. Therefore, Eq. (1) will be solved at first considering only the most important processes, thus fixing the main physical parameters. Successively, all of the other parameters will be adjusted in order to obtain a better agreement with experiments. Indeed, from Eq. (1) both the time resolved and the steady state excited level populations (N_i) can be obtained. The simulated luminescence intensities $I_{s,i}$ coming from the corresponding ith level are simply proportional to the density level population times the radiative rate $w_{R,i}$ of that level, through the following equation:

$$I_{s,i}\propto w_{R,i}N_i. \tag{2}$$

By fitting the experimental intensity data through the simulated intensities given by Eq. (2), fixing the already known constants, we are able to find the unknown physical parameters, such as the coupling costant C_{b1}, describing the Si-NC–Er interaction, or the cooperative up-conversion coefficient C_{up}. A summary of the main physical parameters used in the simulations, which give the best agreement with experimental data, can be found in Table I.

V. THEORY VS EXPERIMENT

In Fig. 3 the total number of photons emitted in steady state conditions at around 1.54 μm (solid triangles) and at around 0.8 μm (solid circles), as deduced from experimental spectra, are reported as a function of Er concentration, for a fixed Si NC concentration of 1×10^{19}/cm^3. In the same figure, the simulated numbers of excited Er ions (open triangles) and Si NC (open circles) calculated from Eq. (1), which are proportional to the numbers of emitted photons at

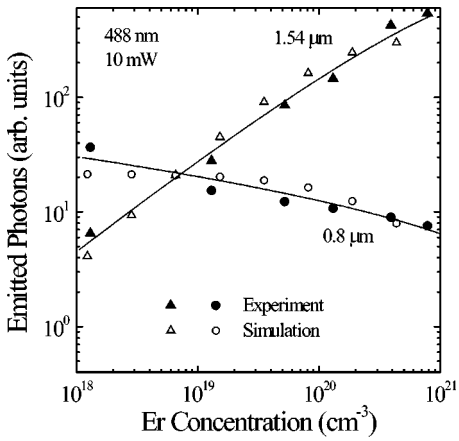

FIG. 3. Comparison between the measured and the simulated integrated numbers of emitted photons at around 1.54 μm (Er-related emission) and 0.8 μm (Si-NC-related emission) as a function of Er concentration. Continuous lines are for guiding the eye.

1.54 and 0.8 μm, respectively, are also plotted for comparison. The continuous lines are just a guide to the eye. It is worth noticing that the agreement between the experimental and the simulated behavior is quite impressive, since we are covering several orders of magnitude by using fixed parameters in the calculations, as reported in Table I. By increasing the Er concentration, the mean number of Er ions per Si NC increases too. When the Er concentration is lower than the NC one, only a few NC's have a nearby Er ion they can couple with. Since the coupling is strong, those NC's, once excited, will preferentially transfer nonradiatively their energy to the neighboring Er ions. Hence for each Er ion coupled to a NC, a photon in the Si NC related spectrum will be lost, and a photon in the Er related spectrum will be gained. The Si NC's which are not coupled to any Er ion continue to emit light at around 0.8 μm with the same lifetime, almost independent of the Er concentration.[28] When the Er concentration equals the Si NC one, every Si NC is coupled with an Er ion, and the Si NC emission is almost completely quenched with respect to the unimplanted sample.[28,31] For Er concentrations greater than the Si NC one, each NC will be surrounded by several Er ions. In principle, due to the strong coupling, each NC is able to excite several Er ions in the typical deexcitation time of the first excited Er level (a few ms), the maximum number being only determined by the excitation rate of the NC, i.e., by the cross section times the incident photon flux, multiplied by the lifetime of the first excited Er level. Since at Er concentrations greater than 2×10^{20}/cm^3 the concentration quenching effect also becomes effective,[30] the Er lifetime will strongly decrease thus producing a reduction of the maximum number of excitable Er ions per NC. This will produce an additional saturation in the high Er concentration side of the 1.54 μm curve in Fig. 3.

In Fig. 4, the Er-related 1.54 and 0.98 μm luminescence intensities, corrected for the system response, are reported as a function of the pump power, varied in the range between 1 and 10^3 mW, for a sample containing 6.5×10^{20} Er/cm^3 in presence of Si NC's. In this wide range, the 1.54 μm inten-

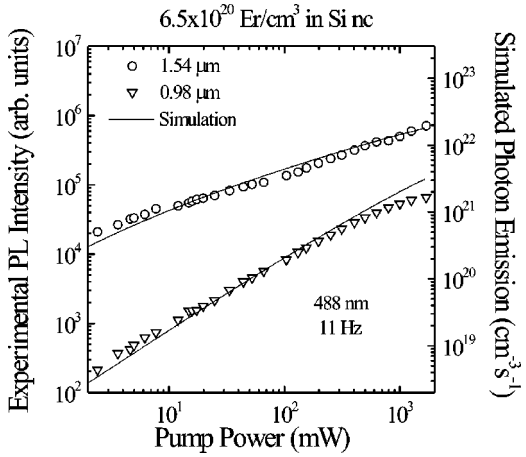

FIG. 4. PL intensities of the 1.54 and 0.98 μm lines as a function of pump power. Continuous lines are the simulated photon emissions as obtained by dividing the density population of the first and second excited Er levels by their respective radiative lifetime (right axis).

sity is seen to strongly saturate, while the 0.98 μm has a linear trend up to 10 mW and then it starts to saturate at higher powers. It is worth noticing that while at low powers the ratio between the 1.54 and 0.98 μm intensities is $\sim 10^2$, at the highest observed powers this ratio strongly reduces to a factor of 10. The continuous lines are fits to the experimental data obtained by solving the rate equations given in Eq. (1) and by using Eq. (2).

To investigate the correlation between the two observed lines, we plotted in Fig. 5 the 0.98 μm luminescence intensity as a function of the 1.54 μm one, for each of the pump

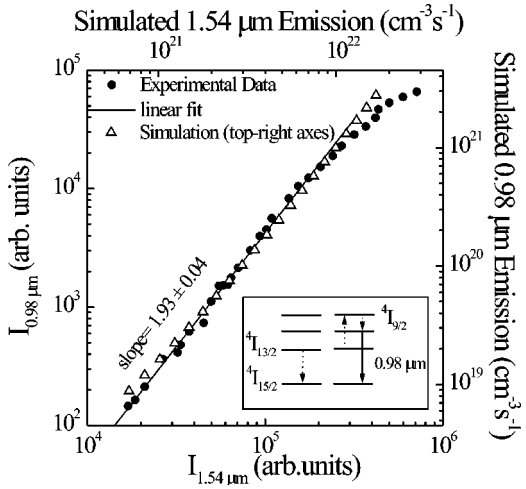

FIG. 5. Correlation graph reporting a quadratic dependence of the 0.98 μm intensity with respect to the 1.54 μm one for the sample containing 6.5×10^{20} Er/cm^3 in presence of Si NC's. Solid circles represent experimental data as extracted from Fig. 4. Open triangles refer to simulated photon emission (top-right axes) as obtained by solving Eq. (1). Inset: schematic diagram showing the cooperative up-conversion mechanism between two interacting Er ions, which determines the emission of a 0.98 μm photon at the expenses of two 1.54 μm photons.

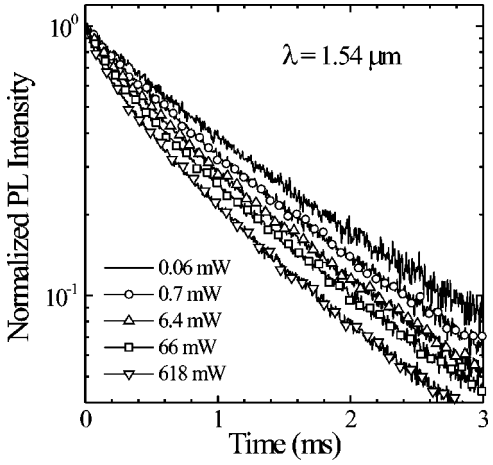

FIG. 6. Time-decay curves recorded at 1.54 μm and at different pump powers for the sample with 6.5×10^{20} Er/cm^3 in presence of Si NC's. The apparent reduction in Er lifetime with increasing pump power is due to the up-conversion mechanism between two excited Er ions which causes the quenching of the 1.54 μm related level in the first instants of the Er deexcitation.

powers used. While the 1.54 μm intensity varies in a range spanning two orders of magnitude, the 0.98 μm line intensity is seen to increase in a three orders of magnitude-wide interval, with a quadratic power law dependence, as attested by the linear fit (continuous line). Once more, the open data represent simulations obtained within the same model. Since the intensity at a certain wavelength is proportional to the number of emitted photons, which is moreover proportional to the number of excited centers emitting at that wavelength, it is possible to conclude that the number of Er ions excited in the $^4I_{11/2}$ level, which is responsible for the 0.98 μm emission, is proportional to the square of the number of Er ions which are excited in the $^4I_{13/2}$ level, i.e., $N_3 \propto N_2^2$. That is to say, in order to have an Er ion excited in the $^4I_{11/2}$ level we need two Er ions excited in the $^4I_{13/2}$ level. This is the result of a typical cooperative up-conversion mechanism, well known for Er in Al_2O_3 (Ref. 44) and in silica glasses,[44,45] which, to our knowledge, had not yet been observed in the Er-doped Si nanocrystals system. As reported in the inset of Fig. 5, in a cooperative up-conversion process, one of two nearby interacting Er ions, both in the first excited state, gives up resonantly and nonradiatively its energy to the other, collapsing to the ground state and bringing the other in the $^4I_{9/2}$ level. Then a nonradiative deexcitation occurs from this level to the lower lying $^4I_{11/2}$ level. Hence, the subsequent radiative recombination from this level produces a 0.98 μm photon. We get a 0.98 μm photon at the expenses of two 1.54 μm photons which can no more be emitted. This is the physical meaning of the quadratic power law behavior observed in Fig. 5.

Other experimental evidences for the occurrence of the cooperative up-conversion mechanism in our Er doped Si NC samples can be gained by looking at the time evolution of the 1.54 μm emission. Indeed, in Fig. 6 time-decay curves recorded at 1.54 μm are reported for different pump powers, normalized to the steady state values. At $t=0$, after the sys-

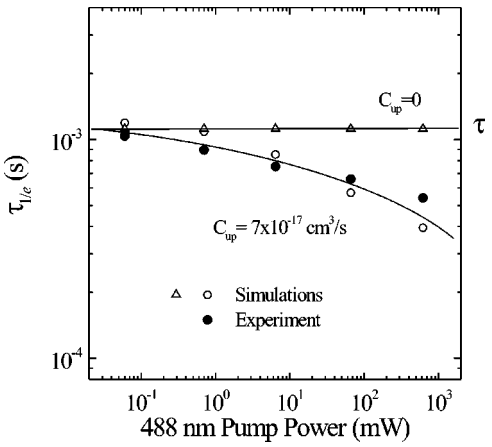

FIG. 7. Comparison between the simulated and experimental e^{-1} mean decay times of the 1.54 μm emission as a function of the excitation power. Experimental data have been extracted from Fig. 6. For a cooperative up-conversion coefficient of 7×10^{-17} cm^3 s^{-1} a good agreement between experiments and simulation can be achieved.

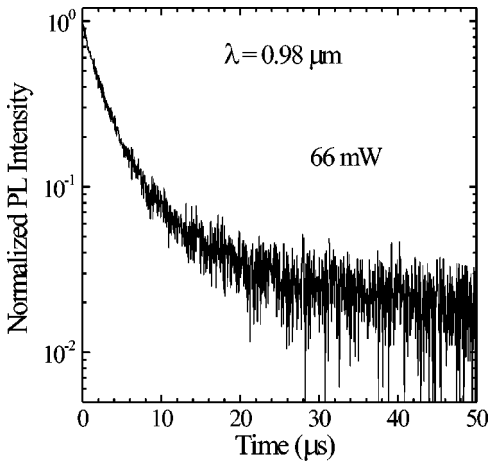

FIG. 8. Time-decay curve of the 0.98 μm emission for a sample containing 6.5×10^{20} Er/cm^3 in presence of Si NC's. The tail which extends for times longer than 10 μs is due to the refilling of the $^4I_{11/2}$ level caused by cooperative upconversion between two Er ions excited both in the long lived $^4I_{13/2}$ level.

tem has reached the steady state condition, we switch off the laser beam and measure the time evolution of the luminescence signal. At very low pump powers the measured lifetime is of the order of 1 ms. Actually this low value is a consequence of the concentration quenching effect taking place in this system.[30] With increasing the pump power, a shortening of the measured lifetime is observed in the first instants of the decay, causing a stretching of the decay curve, which recovers its original straight shape only at longer times. Indeed, with increasing the pump power, the concentration of Er ions brought in the first excited level in steady state conditions increases too. Hence it becomes more probable to find all over the sample pairs of nearby excited Er ions. Within each pair of excited Er ions a strong cooperative up-conversion mechanism sets in, producing a fast quenching of the first excited level population, i.e., of the 1.54 μm luminescence. This quenching continues until excited Er ions remain only far apart, and, being no more interacting, can relax in the ground state emitting photons with the lifetime measured at low pump powers.

In Fig. 7 the experimental e^{-1} lifetime at 1.54 μm measured from Fig. 6 (solid circles) is reported as a function of the pump power used. For comparison, the values simulated by solving the rate equations (1) by using an up-conversion coefficient of 7×10^{-17} cm^3 s^{-1} are also shown (open circles). The agreement is good, considering the wide range of pump powers covered. It is worth noticing that by setting $C_{\rm up}=0$ in Eq. (1) and fixing all of the other parameters, we are not able to take into account the shortening of the lifetime with increasing the pump power (open triangles), demonstrating once more that this reduction is mainly caused by upconversion.

Actually, another mechanism which could in principle produce a shortening of the Er lifetime at 1.54 μm is the Auger effect between an Er ion in its first excited level and an excited NC, represented in Fig. 2 by the coefficient C_A. However, this effect can be ruled out since, in order to take place, a Si NC should remain in its excited state for times as long as the Er lifetime, in order to explain the lifetime shortening at times >100 μs, as shown in Fig. 6. But due to the strong interaction between a Si NC and the nearby Er ions, the lifetime of the exciton in the Si NC has to be much lower than the exciton lifetime in absence of Er, which is ~50 μs. Therefore, once the excitation is switched off, an exciton in presence of Er ions can survive in the NC for times $\ll50$ μs, and it is only in this narrow temporal window that the interaction leading to an Auger quenching process with the first excited level of Er would occur. Therefore, an Auger process would have explained a luminescence quenching at 1.54 μm for times $\ll50$ μs but cannot explain the quenching reported in Fig. 6, since it can be observed even for times >100 μs, i.e., much longer than the typical lifetime of an exciton interacting with Er.

Another direct evidence for the presence of cooperative up conversion can be envisaged in Fig. 8, where a decay-time measurement at the 0.98 μm Er emission is reported, for the very same sample containing 6.5×10^{20} Er/cm^3 and by using a pump power of 66 mW. The 0.98 μm line coming from the radiative recombination of level $^4I_{11/2}$ is characterized by a lifetime of ~2.5 μs, attesting that most of the deexcitations from that level are nonradiative. The decay-time curve reported in Fig. 8 is composed by a first straight part, showing a lifetime of just ~2.5 μs, and of a very long tail extending over 10 μs and characterized by a longer lifetime. Indeed, this long tail is due to the refilling of the $^4I_{11/2}$ at the expenses of level $^4I_{13/2}$ determined by the cooperative upconversion involving two Er ions in the first excited level. Since this level is long-lived, two excited Er ions can interact through upconversion even at times longer than μs, as reported in Fig. 6, thus repopulating the level $^4I_{11/2}$, which otherwise would have been depleted in a mean time of 2.5 μs.

Since we are eventually interested in the emission of a 1.54 μm photon, we want to better investigate the real effect of upconversion in the dynamics of the $^4I_{13/2}$ level popula-

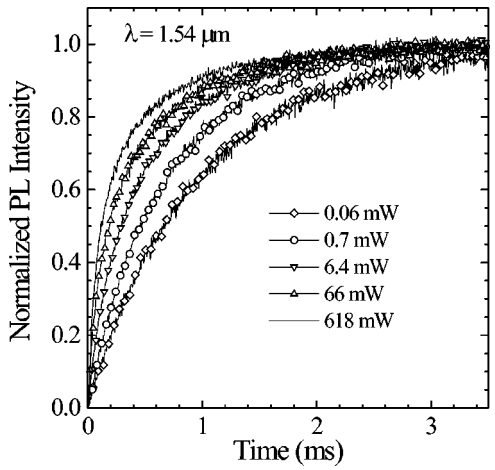

FIG. 9. Time resolved PL intensity at 1.54 μm as a function of the excitation pump power, normalized to the steady state values.

tion. Figure 9 shows the normalized luminescence intensities recorded at 1.54 μm as a function of time after switching on the laser beam at $t=0$, and for different pump powers. As can be observed, the luminescence signal reaches the saturation value in a time which is shorter the higher is the excitation power. We define the typical experimental risetime τ_{on} as the time it takes the luminescence signal to reach the 63% (i.e., $1-e^{-1}$) of the saturation value. In Fig. 10, the reciprocal of the experimental risetime (solid circles) extracted from Fig. 9 is plotted as a function of the pump power. The experimental trend is linear up to 1 mW. Indeed, within this low power regime it is possible to demonstrate that the reciprocal of the risetime τ_{on} follows the law

$$\frac{1}{\tau_{on}} = \sigma_{eff}\phi + \frac{1}{\tau}, \tag{3}$$

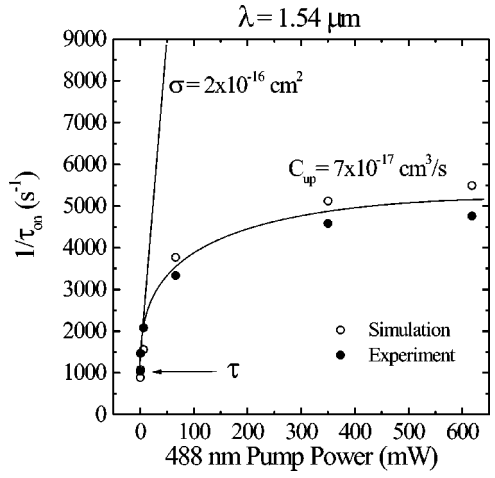

FIG. 10. The reciprocals of the experimental risetimes measured at 1.54 μm are reported as a function of the pump power, as determined from Fig. 9. From a linear fit of the data in the low pumping power regime (up to 1 mW) it is possible to estimate an excitation cross section of $\sim 2\times 10^{-16}$ cm^2 for the Si NC mediated excitation of Er. At higher powers, a strong saturation is observed, due to cooperative upconversion which limits the excitation rate of Er.

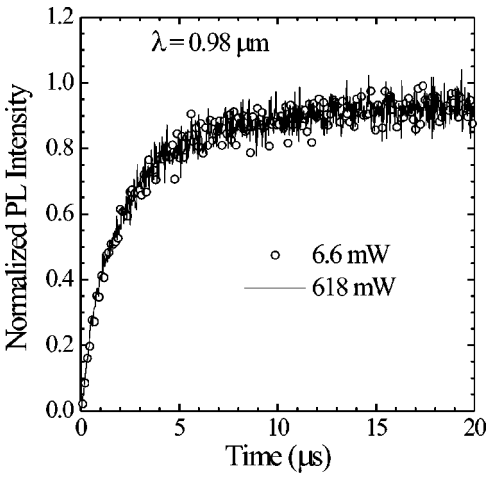

FIG. 11. Photoluminescence intensities at 0.98 μm as a function of time, after switching on the laser excitation at $t=0$ for the sample containing 6.5×10^{20} Er/cm^3 in presence of Si NC's. The mean risetime is independent of the pump power excitation, suggesting that the energy transfer time between Si NC's and Er is actually comparable to the lifetime of level $^4I_{11/2}$, i.e., of the order of ~ 1 μs. The time resolution of our setup is ~ 5 ns.

where ϕ is the photon flux, τ the total lifetime of level $^4I_{13/2}$, comprising the radiative and all the nonradiative deexcitation processes, and σ_{eff} is an effective excitation cross section for Er in presence of Si NC's. From a linear fit of the experimental data through Eq. (3) a value of $\sim 2\times 10^{-16}$ cm^2 can be estimated for the Er excitation cross section, in agreement with recent findings.[30] At higher pump powers, the linear approximation is no more valid, and indeed the trend of the experimental data in Fig. 9 shows a strong saturation, which can be attributed to the up-conversion mechanism, as indicated by the good agreement of the simulated data (open circles) obtained by solving Eq. (1).

Another mechanism which could in principle limit the excitation rate of Er is clearly the transfer mechanism itself. Indeed, given a certain Er concentration, the total number of excitable Er ions depends clearly on the excitation power, but at very high pump powers the effective energy transfer time between a single Si NC and each Er ion becomes the physical limiting factor. In Fig. 11, the luminescence intensity at 0.98 μm is reported as a function of time, normalized for the steady state values, for two very different excitation powers. The mean risetime is clearly independent of the pump power, being equal to 2.4 μs, which is comparable to the decay time of the $^4I_{11/2}$ level. Since this level is directly pumped by a Si NC through a fast decay from level $^4I_{9/2}$, we can conclude that the time it takes a Si NC to transfer its energy to a nearby Er ion must have a typical value of τ_{tr} ~ 1 μs. This means that even if the excitation power is such that more than one exciton is created in each NC in a time interval of 1 μs, only one of these excitons can transfer its energy to the nearby Er ion in that time interval. Therefore increasing the excitation power over a critical value P_c cannot produce a corresponding increase in the excitation rate, thus contributing to the saturation observed in Fig. 10.

In order to estimate the value of the critical power P_c, we need to equal the excitation rate $\sigma_{ab}\phi$ of a NC and the transfer rate $w_{tr}=1/\tau_{tr}$. By using an excitation cross section of 2×10^{-16} cm^2 and a transfer time of 1 μs, we get for the critical photon flux a value $\phi_c=(\sigma_{ab}\tau_{tr})^{-1}=5\times10^{21}$ cm^{-2} s^{-1}. From this critical photon flux value, it is possible to estimate a critical pump power of $P_c=5.7$ W. It is evident from Fig. 10 that the pump power used is well below the critical value P_c. Therefore we conclude that the strong saturation in the excitation rate deduced from Fig. 10 is mainly due to the upconversion mechanism.

At this stage, a few comments need to be made, as far as the efficiency of the energy transfer mechanism itself is concerned. Indeed we can define the efficiency η_{tr} of the transfer mechanism as the ratio between the transfer probability w_{tr}, i.e., the probability per unit time that an exciton generated inside a Si NC gives out its energy to a nearby Er ion in the ground state, and the total recombination probability of the same exciton, comprising both the recombination rate w_b for the isolated NC and the transfer probability. Therefore we get

$$\eta_{tr}=\frac{w_{tr}}{w_{tr}+w_b}. \tag{4}$$

By using the experimentally estimated value of ~1 μs for τ_{tr}, and of 2×10^4 s^{-1} for w_b we get a value of $\sim98\%$ for the energy transfer efficiency, which indeed confirms the strong coupling existing between Si nanocrystals and Er ions.

VI. OPTICAL GAIN

A. Role of Si NC in the Er induced gain

Many parameters can determine and influence a possible optical gain measurement at 1.54 μm in Er-doped Si nanocrystals. Among these, the number of excitable Er ions per nanocrystal clearly deserves great attention. Indeed, in order to reach high material gain values, high concentrations of Er need to be inserted in the sample and moreover in their optically active state. Clearly, if only a small fraction of Er ions is coupled with NC's, all the other Er ions which do not benefit from the sensitizing action of NC's become strongly absorbing. Under these conditions, measuring a positive net gain could become a quite difficult task to achieve, since other processes such as photon absorption from an excited NC, or excited state absorption from the first level of Er will dominate. In this section we want to better investigate problems and perspectives related to optical gain in the Er-doped Si NC system simply extending the simulations obtained through Eq. (1). Indeed, in the previous section the overall experimental data have been fitted through Eq. (1), accurately determining all of the main physical parameters involved. The physical variables that have been varied in the investigation are the Er concentration (ranging between 3×10^{17}/cm^3 and 1.4×10^{21}/cm^3) and the excitation pump power (in the range $1-10^3$ mW). The density of Si nanocrystals in the sample has been fixed to $\sim1\times10^{19}$/cm^3.

In Fig. 12 a contour plot reports in gray scale the simulated number of Er ions excited in the $^4I_{13/2}$ level per Si nanocrystal, in steady state conditions, as a function of both the Er concentration and the power density, obtained by dividing the pump power by the area of the exciting laser spot ($\sim2.8\times10^{-3}$ cm^2). White color indicates the region where less than one Er ion per NC is excited on average. Continuous lines represent constant values. Clearly, for Er concentrations lower than 1×10^{19}/cm^3, the number of excited Er ions per NC cannot exceed 1. When the Er concentration equals the Si NC one, the average number of excited Er ions per NC increases with increasing the pump power, reaching asymptotically the value of 1 at the highest pump powers (vertical dashed line). By increasing the Er concentration, the pump power trend of the number of excited Er ions per NC is still characterized by a saturation behavior, since almost all of the Er ions are excited at the highest power densities. However, the saturation value obtained at very high pump powers increases with the total Er concentration present in the sample, as attested by the brighter tones in the figure. On the other hand, from Fig. 12 we can observe that if the pump power is lower than ~3 W/cm^2, the number of excited Er ions per NC is lower than 1, even at the highest Er concentration used. Indeed, since the excitation of Er through a NC is a sequential process, only one Er ion at a time can be excited by a NC, the typical energy transfer time being very fast, i.e., ~1 μs, as shown before. Therefore, once the NC is excited, it transfers very quickly its energy to a nearby Er ion, thus relaxing to the ground state and waiting for another excitation to occur. If the time inteval $(\sigma_{ab}\phi)^{-1}$ between two successive excitations of a NC is longer than the lifetime τ of the first excited level of Er, in steady state conditions only one Er ion is actually excited per NC, even if a lot of Er ions exists. By letting $\sigma_{ab}\phi=\tau^{-1}$, where $\sigma_{ab}=2\times10^{-16}$ cm^2 and $\tau=2.5$ ms, a critical pump power density value of ~1 W/cm^2 can be estimated, under which the total number of excitable Er ions per NC is limited by the excitation rate of the NC itself. For power densities higher than 3 W/cm^2, the number of excited Er ions per NC increases by increasing the Er concentration, saturating at the highest Er

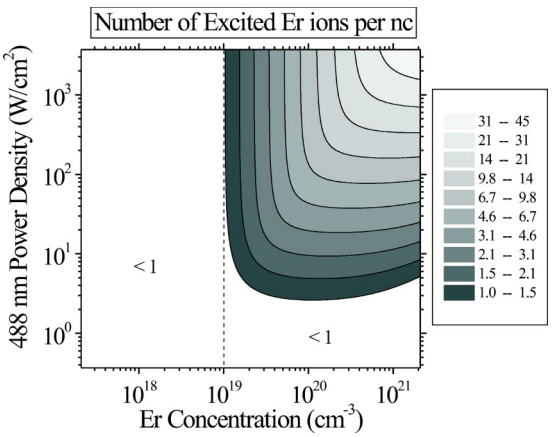

FIG. 12. Contour plot in a logarithmic gray scale showing the number of excited Er ions per Si nanocrystal as a function of the Er concentration and power density, as determined by simulations. The contour lines represent constant values. A large region in the phases space exists where a Si nanocrystal can excite more than one Er ion.

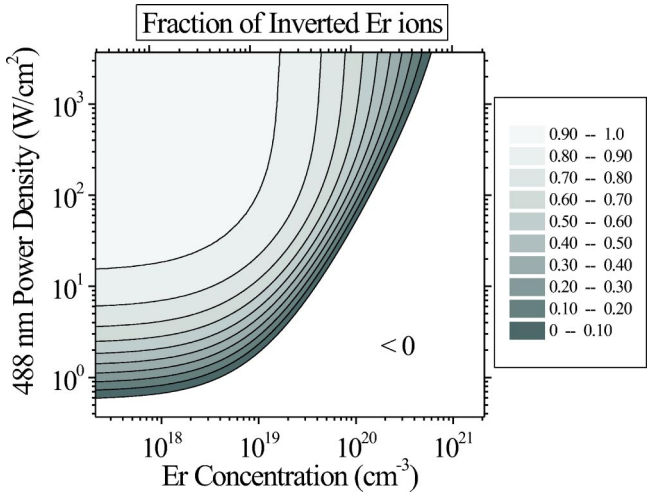

FIG. 13. Contour plot showing the fraction of inverted Er ions as a function of both the Er concentration and pump power density, in a linear gray scale. This fraction decreases both by decreasing the excitation pump power and by increasing the Er concentration in the film.

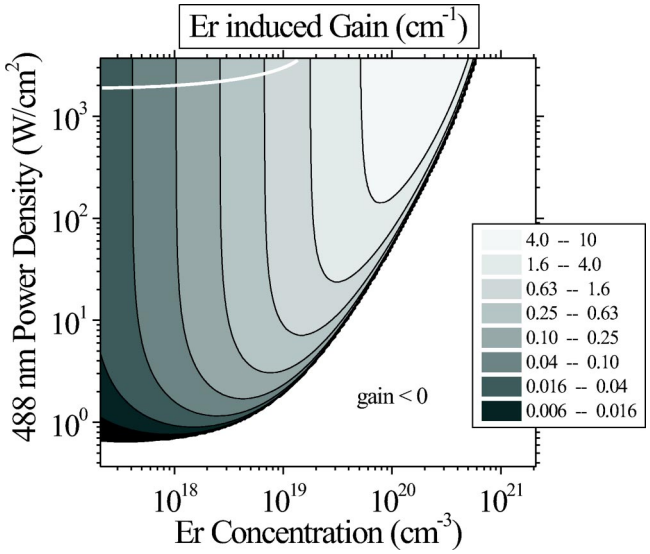

FIG. 14. Contour plot of the Er induced gain at 1.54 μm in Er-doped Si NC's as a function of Er concentration and power density. The white region is for negative gain. The values have been obtained by assuming an Er emission cross section of 1×10^{-19} cm^2, as recently determined by both Kik *et al.* (Refs. 38,39) and Shin *et al.* (Refs. 40–42). The continuous white line represents the zero Er-induced gain threshold curve for Er in SiO_2, without Si NC's (only direct absorption considered).

concentrations to a value which depends on the pump power. This saturation is produced by concentration quenching and up-conversion mechanisms, which are quite effective in the sample. As can be seen, a single Si NC can excite a number as high as 30 Er ions, at the highest pump power and Er concentration used.

It is now interesting to study the Er concentration and the power dependence of the fraction of inverted Er ions in the sample, defined as $(N_2-N_1)/N_0$, where N_2, N_1 are, respectively, the steady state concentrations of Er ions in the first excited level and in the ground state, as determined by solving Eq. (1), and N_0 is the total Er concentration in the film. The results are shown in Fig. 13, where contour lines represent constant values. The white region represents negative values, i.e., noninverted Er ions. For Er concentrations lower than 1×10^{19}/cm^3, 90–100 % of Er ions can be excited at very high pump powers. At a fixed high power density, by increasing the Er concentration, the fraction of inverted Er ions is seen to decrease, due to nonradiative quenching processes, such as concentration quenching and upconversion, which become active for Er concentration greater than $\sim10^{20}$/cm^3 and tend to deplete the first excited level of Er. However, if we look at the gain that can be induced by all of the Er ions present in the matrix, a different scenario appears. Indeed, in Fig. 14 a contour plot showing the Er induced positive gain g at 1.54 μm as a function of both the Er concentration and the pump power is reported in a gray logarithmic scale. The white region is for negative gain. The border line dividing the white and the gray regions is the zero-gain line. Actually $g=\sigma_e(N_2-N_1)$, where σ_e is the emission cross section of level $^4I_{13/2}$, and (N_2-N_1) is the total concentration of Er ions inverted in that level. For the emission cross section of Er, a value of 1×10^{-19} cm^2 has been used, as recently determined by both Kik *et al.*[38,39] and Shin *et al.*[40–42] Figure 14 is quite interesting, since it shows that in order to achieve a positive gain, we need to get across the marked solid curve, delimiting the two regions of positive and negative gain. This is quite similar to a phase transition diagram, where the space coordinates are the Er concentration and the power density, and the two phases are, respectively, the absorbing and the amplifying Er state. Hence the marked line represents the region where both the amplifying and the absorbing phases coexist, i.e., where the material is transparent at 1.54 μm. By increasing the Er concentration, starting from a value of 3×10^{17}/cm^3, the pump power needed to have $g=0$ has to be increased too. It is worth noticing that for Er concentrations higher than the Si NC one, despite quenching processes are limiting the fraction of inverted Er ions, as shown in Fig. 13, positive Er induced gain can still be achieved. In particular, higher Er induced gain can be reached at the highest pump powers and Er concentrations. For example, gain values in between 4 and 10 cm^{-1} can be obtained in a wide region of Er concentration, in the range $5\times10^{19}-6\times10^{20}$/cm^3, but at a power density of about 3.5×10^3 W/cm^2. Clearly, decreasing the power density produces a reduction of the Er concentration window where these gain values can be achieved. Given a certain Er concentration, a critical value of the excitation power exists under which negative losses can only be observed. For example, when the Er concentration is 2×10^{20}/cm^3, a positive Er induced gain could be measured only using power densities greater than $\sim$250 W/cm^2. In addition, a slight increase of the Er concentration produces a strong enhancement, with a quadratic law, of the power threshold, as described by the marked line in Fig. 14.

In Fig. 14, a white line showing the simulated zero-gain curve for Er in SiO_2 without Si NC is also reported. In this

case only excitation of Er through the direct absorption of a 488 nm photon is considered, i.e., the constants C_{bi} describing the coupling between Si NC's and Er ions have been set to zero, while all of the other parameters have been maintained fixed to their original values for simplicity. As can be seen, the power density threshold for observing positive gain is strongly increased, by ~3 orders of magnitude. Thus from Fig. 14 it is evident that Si NC's play a key positive role for the Er induced gain in three main ways. (i) First of all the presence of Si NC's which can strongly absorb the 488 nm incident photons and rapidly transfer the energy to Er, determines a lowering of the pump power threshold needed to observe Er-induced gain, with respect to Er-doped insulating hosts, where only direct photon absorption, characterized by a much lower excitation cross section can occur. (ii) Moreover, Er^{3+} ions in presence of Si NC's can be excited by photons which are not necessarily in resonance with the absorption spectrum of Er^{3+}, since Si NC's can absorb light in a broad spectrum and then transfer quasiresonantly and efficiently their energy to the rare earth. This clearly opens the way towards Er-doped Si-NC-based optical amplifiers pumped by broad band light sources. (iii) Eventually, Si NC's dispersed in the oxide matrix determine both an increase in the mean refractive index and a reduced homogeneity of the material. This produces a greater mixing of the Er related level, and as a consequence, an increase in the radiative transition probability, which reflects in a clear increase of the Er emission cross section.[39,42] Since optical gain is directly proportional to the emission cross section, the Er-doped Si NC offers greater changes to have higher Er induced gain values at 1.54 μm, with respect to insulating hosts.

B. Role of Si NC in the optical losses

Despite the clear positive effects in the Er induced gain, Si NC's could, however, introduce loss mechanisms, which deserve to be studied in details in order to understand the establishment of a net positive gain at 1.54 μm in Er-doped Si nanocrystals. Among these, the most important is surely the confined carriers absorption (CCA) mechanism describing the absorption of a 1.54 μm photon from a confined exciton in a Si NC. This process is the analog of the well known free carrier absorption (FCA) occurring in bulk crystalline Si, where a 1.54 μm photon can be absorbed by a free carrier (both an electron in the conduction band or a hole in the valence band) which is then promoted to a higher excited level. The excitation cross section describing FCA is of the order of 10^{-17} cm^2, while no determination of the CCA cross section is known to our knowledge. In order to study the weight of CCA, we simulated the fraction of excited Si NC's in steady state in our Er-doped Si NC system. By solving Eq. (1) using the coefficients in Table I, we determined the concentration n_b of excited Si NC's. In Fig. 15, the fraction of an excited NC, obtained by dividing n_b for the total NC concentration n_0, is reported as a function of both the Er concentration and the power density, in a gray scale contour plot. This time, increasing values are represented by darker tones of gray. It is worth noticing that when the concentration of Er ions in the film is lower than 10^{19}/cm^3, by increasing the pump power, the fraction of an excited Si NC increases in a way which is almost independent of the particular Er concentration. At the highest pump power used, almost 100% of Si NC's can be excited. When the Er concentration is increased, more than one Er ion can be coupled with a single Si NC, as already reported in Fig. 12. Due to the strong coupling, the contour lines which describe the constant fractions of excited Si NC's bend towards higher pump powers. Indeed a wide region opens up (represented by white), where less than 10% excited NC exists in the film. This is a region where losses induced by CCA from an excited Si NC can be so low to allow for a good chance in observing positive gain.

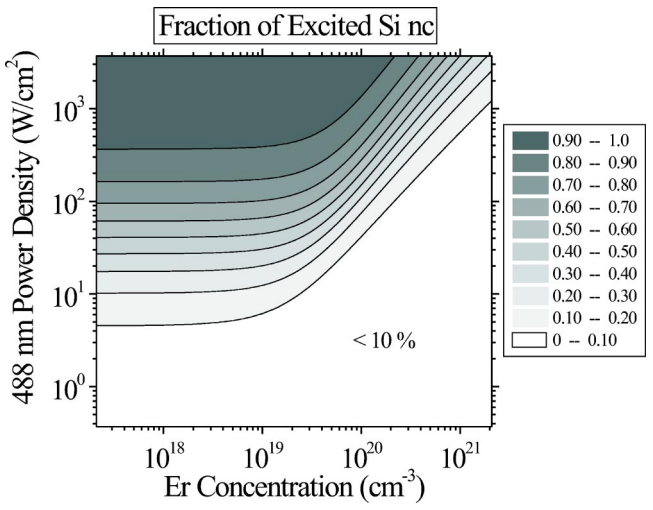

FIG. 15. Contour plot showing the fraction of excited Si nanocrystals as a function of both the Er concentration and the pump power, as obtained by simulations.

In order to compare the strength of both the Er induced gain g and the Si-NC-induced losses α_{CCA}, we define a parameter ρ as the ratio

$$\rho = \frac{g}{\alpha_{\mathrm{CCA}}} = \frac{\sigma_e(N_2 - N_1)}{\sigma_{\mathrm{CCA}} n_b}, \tag{5}$$

where σ_{CCA} is the confined carriers absorption cross section. In order to have a positive net gain, we should have $\rho > 1$. In Fig. 16 the ratio between the concentration of inverted Er ions (i.e., $N_2 - N_1$) and the concentration of excited Si NC's (i.e., n_b) is reported as a function of pump power and Er concentration. A wide region in the phase space exists where $(N_2 - N_1)/n_b > 1$. In this region a net positive gain would be observed only if $\sigma_e/\sigma_{\mathrm{CCA}} \geqslant 1$, since in this case $\rho > 1$ too. But this is a quite lucky situation, where we are assuming that the emission process from an excited Er ion has the same (or higher) strength than the carrier absorption from an excited Si NC. Unfortunately, this turns to be untrue to some extent. For example in bulk Si the free carrier absorption cross section is more than two orders of magnitude higher with respect to the emission cross section of Er. However,

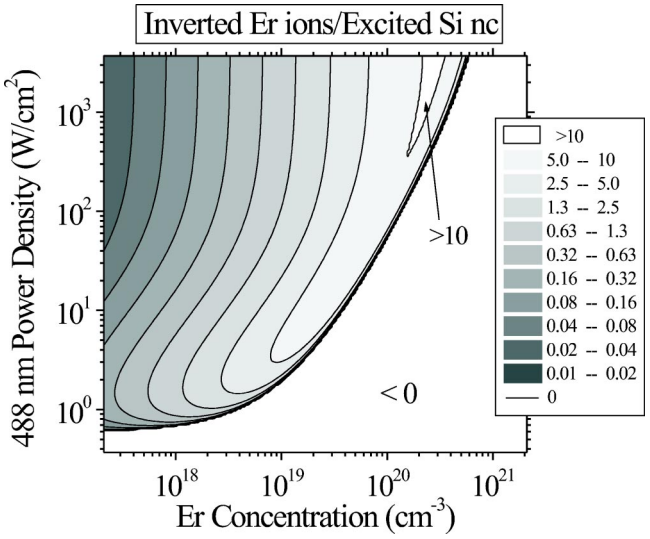

FIG. 16. Contour plot for the ratio between the concentration of inverted Er ions and the concentration of excited Si nanocrystals versus the Er concentration and the pump power density. The region in the phase space where an effective gain can be observed depends on the effective ratio between the emission and the confined carriers absorption cross sections.

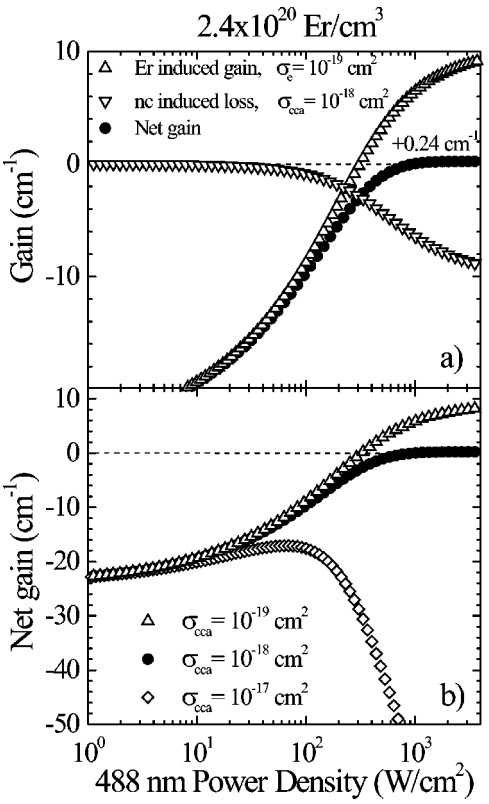

FIG. 17. (a) Er induced gain (up triangles), Si nanocrystals induced loss (down triangles) due to absorption from a confined exciton, and effective gain (closed circles) for a sample containing $2.4\times10^{20}/\mathrm{cm}^3$ Er ions, as a function of the excitation power density. A positive net gain of 0.24 cm^{-1} can be observed at high pump powers. (b) Net gain for three different values of the confined carriers absorption coefficient.

recent experiments suggest that carrier absorption from Si NC could be somewhat reduced with respect to bulk Si (Ref. 39), being characterized by an absorption cross section of $\sim10^{-18}$ cm^2. Therefore, assuming this value, we get $\sigma_e/\sigma_{\mathrm{CCA}}=10^{-1}$. Hence a net positive gain could be achieved only when $(N_2-N_1)/n_b>10$, as reported in Fig. 16.

In Fig. 17(a), the Er induced gain g (up triangles), the Si NC induced losses α_{cca} (down triangles) and the effective gain $g_{\mathrm{net}}=g-\alpha_{\mathrm{CCA}}$ (closed circles) are shown as a function of the excitation power, for an Er concentration of $2.4\times10^{20}/\mathrm{cm}^3$. For very high pump powers, the simulated net gain is 0.24 cm^{-1}. This positive gain is a result of the sensitizing action played by Si NC's in exciting Er ions. Indeed, since each NC is able to excite more than one Er ion, the material gain can be so high to overcome the Si NC induced losses. Moreover, due to the strong interaction between NC and Er, the energy transfer time can be so fast to strongly reduce the fraction of excited Si NC's, thus lowering the NC induced losses. Higher gain values could be obtained increasing the coupling coefficient between NC and Er and reducing the up-conversion mechanism, by playing both with the material used and with the preparation conditions. However, an accurate determination of the confined carriers absorption cross section is still necessary, since as reported in Fig. 17(b) the actual value of this parameter strongly influences the net gain of the Er-Si NC system. Indeed, from the figure it can be noticed that the system can have quite high gain values (~10 cm^{-1}) if $\sigma_{\mathrm{CCA}}=1\times10^{-19}$ cm^2, while it turns to be strongly absorbing if the CCA cross section tends towards the bulk-Si value of 1×10^{-17} cm^2. The recent experimental observation[40–42] of net optical gain in the system is a clear proof that CCA should be quite reduced with respect to the bulk Si value.

VII. CONCLUSIONS

In conclusion, we have presented a phenomenological description of the Er-doped Si nanocrystals system able to quantitatively describe the measured optical properties. By introducing a rate equation based formalism, describing the density populations of interacting Si-NC–Er levels, we were able to determine both the NC-Er coupling constant and the up-conversion coefficient, through a fit of the overall experimental data. Moreover, an energy transfer time of ~1 μs has been experimentally estimated. It has been demonstrated that each Si nanocrystal can be coupled with more than one Er ion, the maximum number of excitable Er ions per nanocrystal being only limited by the Si NC excitation rate, by the total Er concentration, given a fixed NC concentration, and eventually by the transfer time. The possibility of observing positive gain at 1.54 μm in such a system has been extensively discussed, with a particular attention to gain limiting effects, such as cooperative upconversion and confined carriers absorption induced by excited nanocrystals. Indeed we

have shown that Si NC's can have positive as well as negative aspects as far as the optical gain at 1.54 μm from Er-doped Si NC is concerned. Nevertheless, under appropriate conditions net optical gain can be reached. All of these studies, together with our recent demonstration of the feasibility of electrical pumping,[37] open the route towards the possibility of fabricating electrically driven optical amplifiers based on the promising Er-doped Si nanocrystals system.

ACKNOWLEDGMENTS

The authors wish to thank Alessia Irrera for useful discussions, Natale Marino, Antonio Marino, Salvo Pannitteri, and Aldo Spada for their expert technical collaboration. This work has been partially supported by EU through the IST-SINERGIA project, by INFM through the project RAMSES, and by MIUR through the project FIRB.

[1] L. T. Canham, Appl. Phys. Lett. **57**, 1046 (1990).
[2] A. G. Cullis, L. T. Canham, and P. D. J. Calcott, J. Appl. Phys. **82**, 909 (1997), and references therein.
[3] Y. Kanemitsu, T. Ogawa, K. Shiraishi, and K. Takeda, Phys. Rev. B **48**, 4883 (1993).
[4] T. Shimizu-Iwayama, K. Fujita, S. Nakao, K. Saitoh, T. Fujita, and N. Itoh, J. Appl. Phys. **75**, 7779 (1994).
[5] J. G. Zhu, C. W. White, J. D. Budai, S. P. Withrow, and Y. Chen, J. Appl. Phys. **78**, 4386 (1995).
[6] K. S. Min, K. V. Shcheglov, C. M. Yang, H. A. Atwater, M. L. Brongersma, and A. Polman, Appl. Phys. Lett. **69**, 2033 (1996).
[7] M. L. Brongersma, A. Polman, K. S. Min, E. Boer, T. Tambo, and H. A. Atwater, Appl. Phys. Lett. **72**, 2577 (1998).
[8] V. I. Klimov, Ch. Schwarz, D. McBranch, and C. W. White, Appl. Phys. Lett. **73**, 2603 (1998).
[9] T. Shimizu-Iwayama, N. Kunumado, D. E. Hole, and P. Townsend, J. Appl. Phys. **83**, 6018 (1998).
[10] J. Linnros, N. Lalic, A. Galeckas, and V. Grivickas, J. Appl. Phys. **86**, 6128 (1999).
[11] F. Iacona, G. Franzò, and C. Spinella, J. Appl. Phys. **87**, 1295 (2000).
[12] Z. H. Lu, D. J. Lockwood, and J.-M. Baribeau, Nature (London) **378**, 258 (1995).
[13] D. J. Lockwood, Z. H. Lu, and J. M. Baribeau, Phys. Rev. Lett. **76**, 539 (1996).
[14] V. Vinciguerra, G. Franzò, F. Priolo, F. Iacona, and C. Spinella, J. Appl. Phys. **87**, 8165 (2000).
[15] P. Photopoulos, A. G. Nassiopoulou, D. N. Kouvatsos, and A. Travlos, Appl. Phys. Lett. **76**, 3588 (2000).
[16] P. D. J. Calcott, K. J. Nash, L. T. Canham, M. J. Kane, and D. Brumhead, J. Phys.: Condens. Matter **5**, L91 (1993).
[17] M. Brongersma, P. G. Kik, A. Polman, K. S. Min, and H. A. Atwater, Appl. Phys. Lett. **76**, 351 (2000).
[18] K. S. Zhuravlev and A. Yu. Kobitski, Semiconductors **34**, 1203 (2000).
[19] A.Yu. Kobitski, K. S. Zhuravlev, H. P. Wagner, and D. R. T. Zahn, Phys. Rev. B **63**, 115423 (2001).
[20] M. V. Wölkin, J. Jorne, P. M. Fauchet, G. Allan, and C. Delerue, Phys. Rev. Lett. **82**, 197 (1999).
[21] F. Priolo, G. Franzò, S. Coffa, and A. Carnera, Phys. Rev. B **57**, 4443 (1998).
[22] G. Franzò, F. Priolo, S. Coffa, A. Polman, and A. Carnera, Appl. Phys. Lett. **64**, 2235 (1994).
[23] S. Coffa, G. Franzò, and F. Priolo, Appl. Phys. Lett. **69**, 2077 (1996).
[24] A. J. Kenyon, P. F. Trwoga, M. Federighi, and C. W. Pitt, J. Phys.: Condens. Matter **6**, L319 (1994).
[25] M. Fujii, M. Yoshida, Y. Kanzawa, S. Hayashi, and K. Yamamoto, Appl. Phys. Lett. **71**, 1198 (1997).
[26] M. Fujii, M. Yoshida, S. Hayashi, and K. Yamamoto, J. Appl. Phys. **84**, 4525 (1998).
[27] T. Komuro, T. Katsumata, T. Morikawa, X. Zhao, H. Isshiki, and Y. Aoyagi, Appl. Phys. Lett. **74**, 377 (1999).
[28] G. Franzò, V. Vinciguerra, and F. Priolo, Appl. Phys. A: Mater. Sci. Process. **69**, 3 (1999).
[29] G. Franzò, F. Iacona, V. Vinciguerra, and F. Priolo, Mater. Sci. Eng., B **69/70**, 338 (1999).
[30] F. Priolo, G. Franzò, D. Pacifici, V. Vinciguerra, F. Iacona, and A. Irrera, J. Appl. Phys. **89**, 264 (2001).
[31] G. Franzò, D. Pacifici, V. Vinciguerra, F. Iacona, and F. Priolo, Appl. Phys. Lett. **76**, 2167 (2000).
[32] P. G. Kik, M. L. Brongersma, and A. Polman, Appl. Phys. Lett. **76**, 2325 (2000).
[33] P. G. Kik and A. Polman, J. Appl. Phys. **88**, 1992 (2000).
[34] S. -Y. Seo and J. H. Shin, Appl. Phys. Lett. **78**, 2709 (2001).
[35] K. Watanabe, M. Fujii, and S. Hayashi, J. Appl. Phys. **90**, 4761 (2001).
[36] F. Priolo, G. Franzò, F. Iacona, D. Pacifici, and V. Vinciguerra, Mater. Sci. Eng., B **81**, 9 (2001).
[37] F. Iacona, D. Pacifici, A. Irrera, M. Miritello, G. Franzò, F. Priolo, D. Sanfilippo, G. Di Stefano, and P. G. Fallica, Appl. Phys. Lett. **81**, 3242 (2002).
[38] P. G. Kik and A. Polman, J. Appl. Phys. **91**, 534 (2002).
[39] P. G. Kik *et al.* (unpublished).
[40] H.-S. Han, S.-Y. Seo, and J. H. Shin, Appl. Phys. Lett. **79**, 4568 (2001).
[41] H.-S. Han, S.-Y. Seo, J. H. Shin, and N. Park, Appl. Phys. Lett. **81**, 3720 (2002).
[42] J. H. Shin *et al.* (Ref. 39).
[43] D. Pacifici, E. C. Moreira, G. Franzò, V. Martorino, F. Priolo, and F. Iacona, Phys. Rev. B **65**, 144109 (2002).
[44] G. N. van den Hoven, E. Snoeks, A. Polman, C. van Dam, J. W. M. van Uffelen, and M. K. Smit, J. Appl. Phys. **79**, 1258 (1996).
[45] A. Polman, J. Appl. Phys. **82**, 1 (1997).